

**KERNFORSCHUNGSZENTRUM**

**KARLSRUHE**

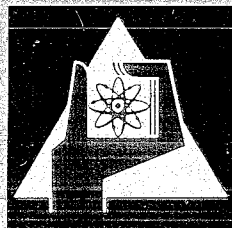
April 1970

KFK 1189

Institut für Angewandte Kernphysik

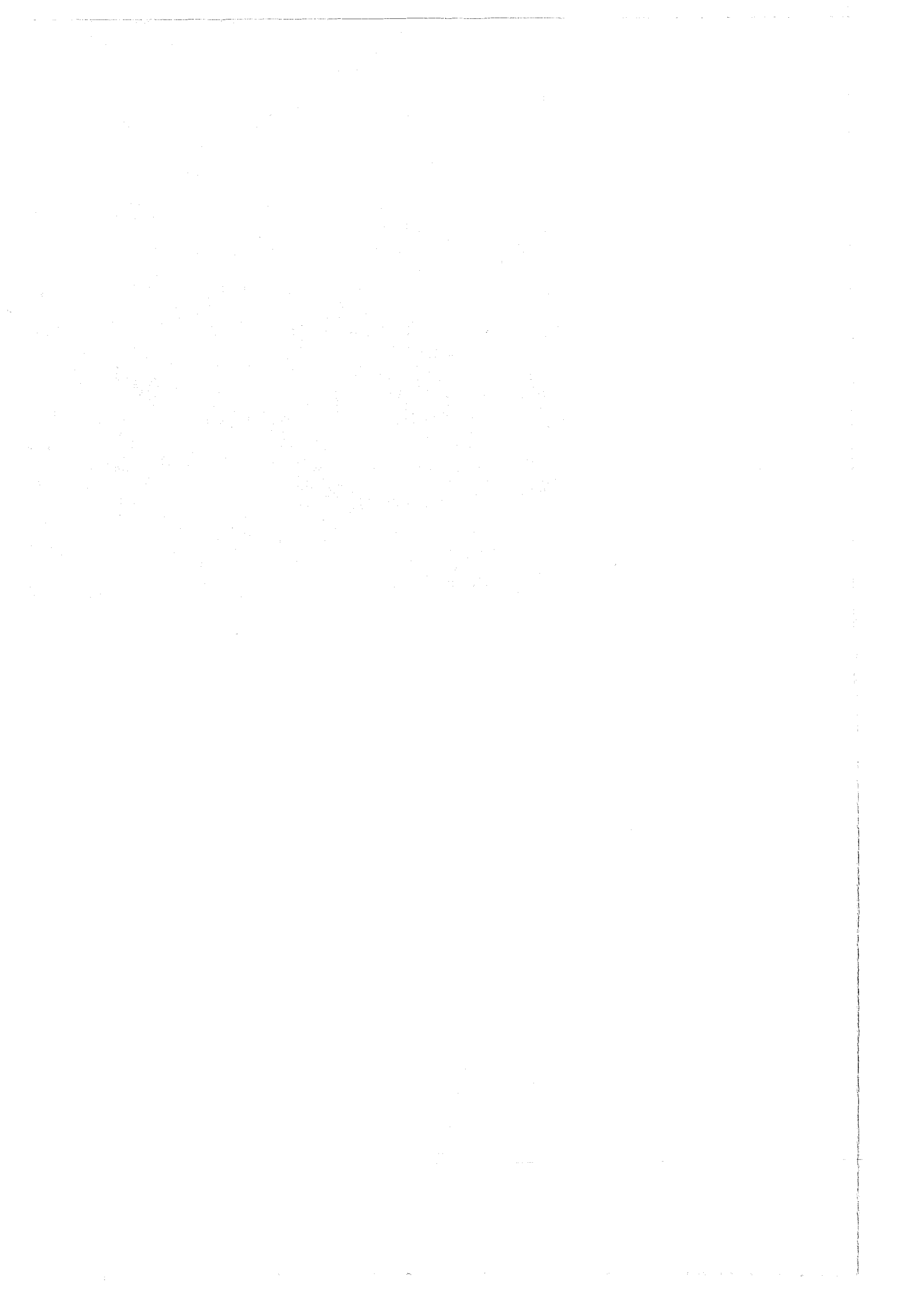
High Resolution Neutron Scattering Measurements and the  
Analysis of Resonance Angular Momentum and Parity

J. Nebe, G.J. Kirouac



GESELLSCHAFT FÜR KERNFORSCHUNG M. B. H.

KARLSRUHE



KERNFORSCHUNGSZENTRUM KARLSRUHE

April 1970

KFK 1189

Institut für Angewandte Kernphysik

High Resolution Neutron Scattering Measurements and the  
Analysis of Resonance Angular Momentum and Parity

J. Nebe and G. J. Kirouac

A paper submitted to the Joint Spring Meeting of the  
German and Dutch Physical Societies

Eindhoven, Netherlands, April 1970

Gesellschaft für Kernforschung m.b.H., Karlsruhe

THE UNIVERSITY OF CHICAGO

1950

CHICAGO, ILLINOIS

TO THE PRESIDENT OF THE UNIVERSITY OF CHICAGO

FROM THE FACULTY OF THE DIVISION OF THE PHYSICAL SCIENCES

RESOLUTION OF THE FACULTY OF THE DIVISION OF THE PHYSICAL SCIENCES

APPROVED BY THE FACULTY OF THE DIVISION OF THE PHYSICAL SCIENCES

## Abstract

This report is taken directly from a talk given at the 1970 Joint Spring Meeting of the German and Dutch Physical Societies held in Eindhoven, Netherlands. As a result of the interest demonstrated in this work, we have published it here.

The talk demonstrates the assignment of neutron resonance spins and parities by direct examination of the differential scattering spectrum shape as a function of energy at a few scattering angles. The test case shown here concerns the well known  $^{12}\text{C}$  (n,n) scattering cross section in the energy range 2 to 6 MeV. Some of our highly structured  $^{40}\text{Ca}$  scattering data are also shown. Detailed analysis of the calcium data is nearly completed and will be reported soon.

Dieser Bericht ist ein Konferenzbeitrag zur Frühjahrstagung der Deutschen Physikalischen Gesellschaft, vorgetragen im April 1970 in Eindhoven, Holland. Wegen des allgemeinen Interesses an dieser Arbeit wird der Vortrag an dieser Stelle veröffentlicht.

Es wird eine Methode erläutert, die es ermöglicht, aus der Form des differentiellen Streuquerschnitts bei wenigen Winkeln Spins und Paritäten von Neutronenresonanzen zuzuordnen. Diese Methode wird am Beispiel der differentiellen Streudaten von  $^{12}\text{C}$  im Energiebereich von 2 bis 6 MeV veranschaulicht. Für  $^{40}\text{Ca}$  wird ein Teil unserer hoch aufgelösten differentiellen Streuquerschnitte gezeigt, deren komplizierte Niveau-Struktur nach der diskutierten Methode analysiert werden. Eine vollständige Analyse der Ca-Daten ist fast abgeschlossen und wird in Kürze veröffentlicht werden.

The first part of the document discusses the importance of maintaining accurate records of all transactions. It emphasizes that every entry should be supported by a valid receipt or invoice. This ensures transparency and allows for easy verification of the data.

Additionally, it is noted that regular audits are essential to identify any discrepancies or errors early on. This proactive approach helps in maintaining the integrity of the financial statements and prevents any potential issues from escalating.

The document also highlights the need for clear communication between all parties involved. Regular meetings and reports should be used to keep everyone informed about the current status and any changes that may occur.

In conclusion, the document serves as a comprehensive guide for managing financial records effectively. By following the outlined procedures, organizations can ensure that their data is accurate, secure, and easily accessible.

It is recommended that these guidelines be reviewed periodically to adapt to any changes in regulations or internal policies. This will help in maintaining the highest standards of financial management.

The document is intended to provide a clear and concise overview of the required processes, ensuring that all staff members are well-informed and capable of performing their duties accurately.

The work reported here is part of a program whose main aim is the study of fast neutron resonances. During the course of these investigations, spin and parity assignment of narrow, closely spaced resonances proved to be a problem of considerable difficulty. For the determination of these parameters, high resolution neutron scattering data have recently been measured. Hitherto the method of phase shift analysis has been applied for the evaluation of such data. This method has been very successful in describing broad structure and energy regions where phase shifts for only a few  $l$ -values are involved. For the present case, this method is of limited application since resonances are closely spaced and uniqueness is difficult to obtain. This difficulty can be overcome by a detailed study of resonance shapes and symmetries in the differential elastic scattering cross sections. With high resolution, the analysis of scattering data can be performed by a direct shape comparison between theory and experiment.

It is this method which will be discussed here. For illustration, high resolution neutron scattering data on carbon are presented. These data have been measured in the energy range from 550 keV to 6 MeV using the neutron time-of-flight facility at the Karlsruhe isochronous cyclotron. A broad neutron spectrum was produced by bombarding a uranium target with deuterons of the internal cyclotron beam. The data recording system included four proton recoil detectors, a detector position coder and a digital time analyzer coupled to an on-line computer. Standard time-of-flight techniques were used for data collection. For a 58 m light path, a resolution of .05 nsec/m was achieved. This corresponds to an energy resolution of 700 eV at 550 keV and of 25 keV at 6 MeV.

Figure 1 gives a view of the main part of the experimental set-up. An aluminum collimator was used at the end of the flight path. The scattering samples were cylinders with symmetry axes perpendicular to the reaction plane. The sample was viewed by three neutron detectors each subtending an angle of  $25^\circ$ . A small plastic

scintillator in the open beam direction served as a neutron flux detector. Data were simultaneously taken at angles of  $54^\circ$ ,  $90^\circ$ ,  $140^\circ$  and at  $0^\circ$  for flux monitoring. The choice of these angles is based on the analysis method which utilizes the angular dependence of resonance shapes in the elastic scattering cross section. These cross section shapes are very sensitive to the  $l$ -value of a resonance state due to the interference between resonance scattering and hard sphere scattering from other partial waves. Thus, a few properly chosen angles allow a unique determination of the  $l$ - and  $J$ -value. Using the Legendre polynomial expansion and the R-matrix formalism, a set of characteristic resonance shapes has been calculated.

Figure 2 shows a set of single level shapes for  $s$ ,  $p$  and  $d$  wave resonances at the three angles chosen in the experiment. The calculations were performed for a hypothetical  $^{12}\text{C}$  resonance at 4 MeV with a width of 200 keV. A nuclear radius of 3.3 fermi was assumed. Contributions of partial waves through  $l = 4$  were included in the representation of the scattering. In view of the different shapes the main features for level identification can be seen.

Since for  $s$ -waves the dominant part in the interference cross section is contributed by the  $L = 0$  term in the Legendre expansion, there is no pronounced angular dependence. The decrease of the cross section maximum for  $90^\circ$  and the shift at backward angles are typical and can be explained by the  $s$ -wave resonance -  $p$ -wave potential interference via the  $L = 1$  term.

For  $p$ -waves a symmetry at  $90^\circ$  is apparent. This is produced by the disappearance of  $s$ -wave potential -  $p$ -wave resonance interference contained in the  $L = 1$  term of the Legendre expansion. A destructive interference below resonance and a constructive above are seen at forward angles. This effect is reversed at backward angles and is common to both  $J$ -values. The different

amplitude behaviour - the steady decrease for  $p\ 1/2$  and the slight increase at backward angles for  $p\ 3/2$  - allows spin identification.

A d-wave resonance can be identified from the sharp amplitude increase at backward angles. The d-wave character is confirmed by the distinct d-wave resonance - s-wave potential interference pattern which goes through zero at  $54.7^\circ$  and  $125.3^\circ$ , the zeros of the second Legendre polynomial.

The general appearance of such resonance shapes is largely independent of energy and channel radius varying only in details of magnitude. Significant shape changes are seen from coherence effects. Figure 3 illustrates such effects which occur in the differential scattering cross section for resonances of both same and different spin and parity. For demonstration, d-wave resonances 20 keV and 300 keV wide of  $J = 3/2$  were chosen. The narrow resonance was moved across the broad state fixed at 4 MeV in order to investigate shape distortions due to interference. This effect is evident on the deep minimum between the resonances. Many such calculations were performed for s, p and d waves with various J-values. They form a family of standard resonance shapes which can be referred to during comparison against measured data.

To demonstrate the practicability of level assignment from a direct study of resonance shapes, carbon elastic scattering data are shown in Figure 4. The spins and parities for the first four levels in  $^{12}\text{C}$  are well known from previous analyses. These data were measured in order to normalize our other scattering measurements to the cross section of carbon below 2 MeV. The values shown were calculated directly from the scattering yield. The calculation involved corrections for flux attenuation in the sample.

No corrections were applied for multiple scattering and angular resolution. The statistical error is less than 2 % and does not exceed the point size. The assignment of  $l$  and  $J$  values is made by reference to the precalculated standard shapes and characteristic

features of s, p and d wave resonances. Thus, two d  $3/2$  resonances are assigned at 2.95 and 3.67 MeV with non-negligible resonance-resonance interference. The lowest level is in accordance with a narrow d  $5/2$  resonance. The resonances at 4.2 and 5.35 MeV correspond to p-waves with spin  $1/2$  and  $3/2$ , respectively. The lower part of the figure shows the theoretical shape of the cross section based on these assignments. This shape is in good agreement with the experimental data. Complete agreement is also found with previous spin and parity assignments.

Having thus examined the reliability of direct shape analysis, application to extremely narrow and closely spaced resonance structure is intended. Figure 5 shows a portion of our calcium differential neutron scattering cross section which is currently undergoing evaluation. The absolute values shown are estimated to be accurate within 15 %. Direct comparisons with other data are difficult due to the lack of equivalently high resolution. The present data, averaged over 130 keV, agree well with the BNL 400 values reported by Langsdorf. Nearly all resonances seen in the energy range from 750 keV to 1.15 MeV could be assigned unambiguously. Further details of our analysis will be given in a later report.

Summarizing, we conclude that detailed study of resonance shapes observed at a few angles can be used to advantage for the assignment of spins and parities even for closely spaced interfering resonances.

Figure Captions

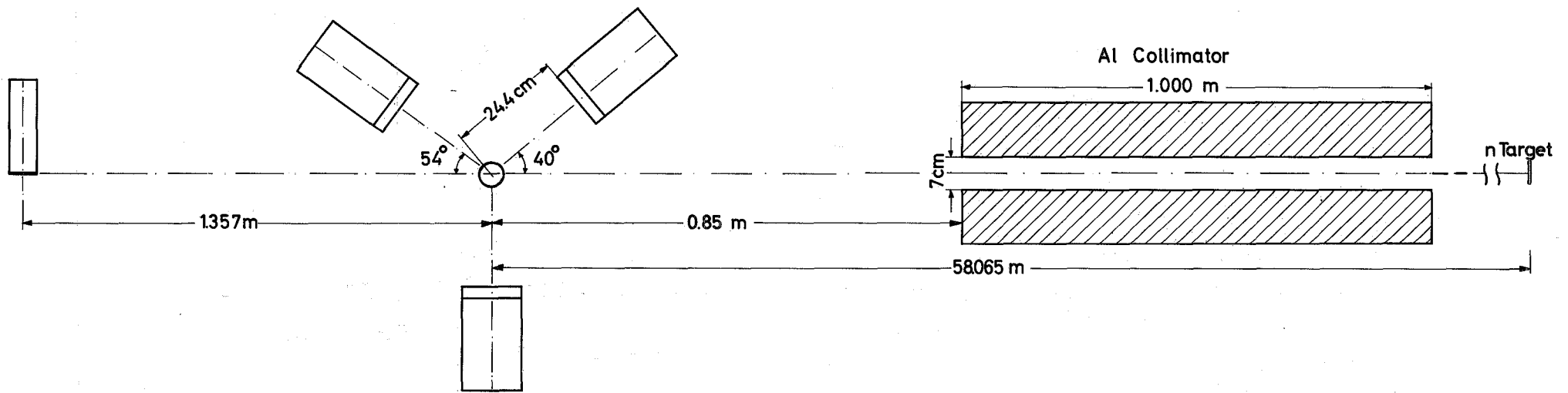
- Fig. 1 Geometry for Elastic Neutron Scattering Experiment
- Fig. 2 Examples of Isolated s, p and d-wave Resonance Shapes for  $^{12}\text{C}(n,n)$
- Fig. 3 Illustration of Coherent Interference between Levels with same Spin and Parity  $3/2^+$
- Fig. 4 Experimental and Calculated Scattering Data for  $^{12}\text{C}(n,n)$  between 2 and 6 MeV
- Fig. 5 Differential Neutron Scattering Cross Section for  $^{40}\text{Ca}$  between 750 keV and 1.15 MeV

1. The first part of the document discusses the importance of maintaining accurate records of all transactions. It emphasizes that proper record-keeping is essential for the integrity of the financial system and for the ability to detect and prevent fraud. The text notes that without reliable records, it would be difficult to verify the accuracy of financial statements and to identify any discrepancies or irregularities.

2. The second part of the document focuses on the role of internal controls in ensuring the accuracy and reliability of financial information. It describes how internal controls are designed to prevent errors and fraud, and to ensure that all transactions are properly authorized and recorded. The text highlights the importance of a strong internal control system in maintaining the trust of investors and other stakeholders in the financial statements of a company.

3. The third part of the document discusses the importance of transparency and disclosure in financial reporting. It notes that providing clear and concise information about a company's financial performance and position is crucial for investors and other users of financial statements. The text emphasizes the need for companies to disclose all material information, including any risks and uncertainties, in a timely and accurate manner.

4. The fourth part of the document discusses the importance of the audit process in providing an independent and objective assessment of a company's financial statements. It notes that audits are conducted by independent auditors who are not affiliated with the company being audited, and who are responsible for expressing an opinion on the accuracy and reliability of the financial statements. The text highlights the importance of a strong audit process in providing confidence to investors and other stakeholders in the financial statements of a company.



Scintillator - Plastic	NE - 102A	11.43 cm x 2.54 cm
Monitor Scintillator -	NE - 102A	2.54 cm x 0.635cm
Photomultipliers -	VALVO	XP - 1040
Monitor Phototube -	VALVO	56AVP
Sample -	5 cm dia x 12 cm	

Fig.1 Experimental Geometry

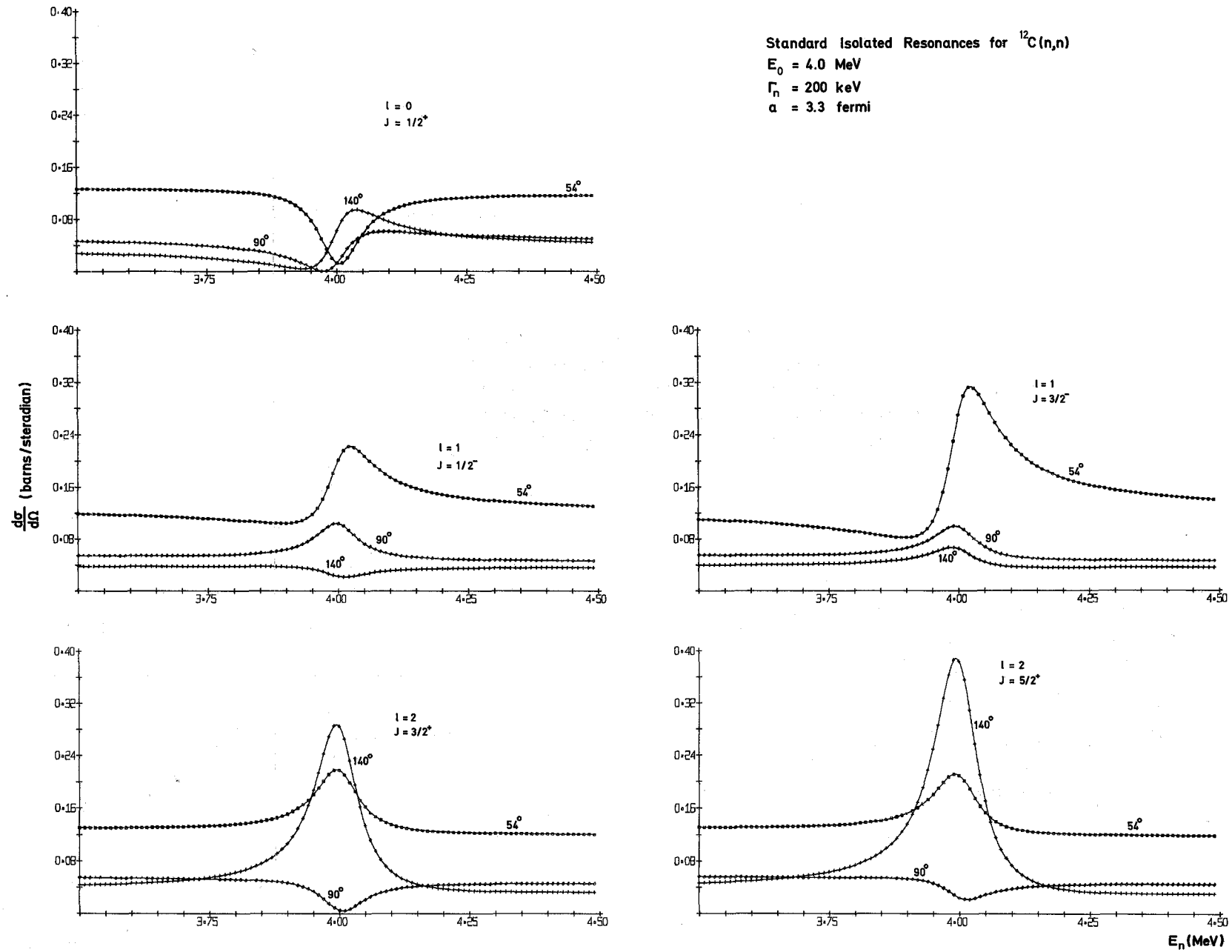


Fig.2 Standard Isolated Resonance Shapes for s.p and d waves

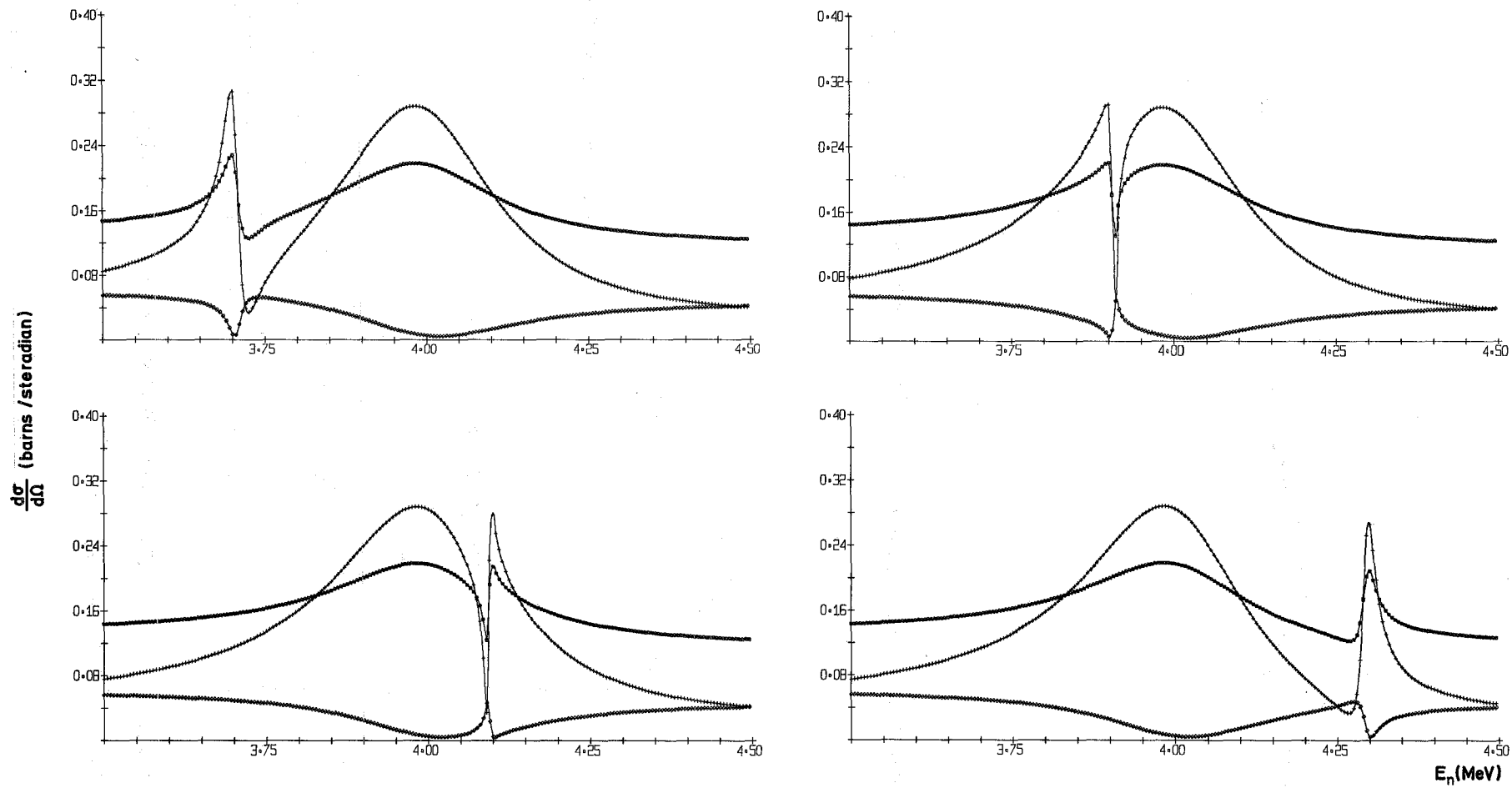


Fig. 3 Interference Effects between two Resonances with Spin and Parity  $3/2^+$

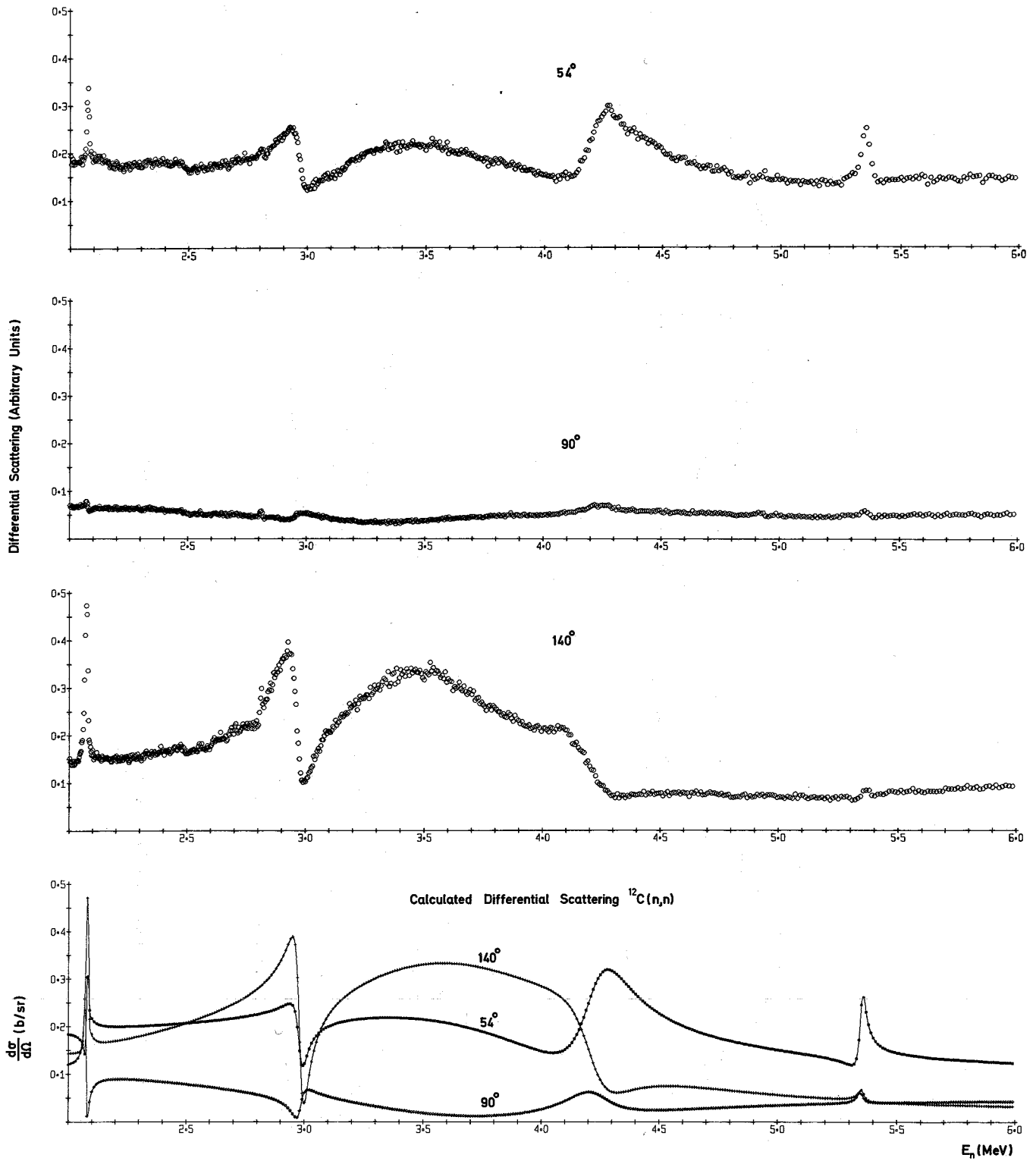


Fig.4 Experimental and Calculated Differential Scattering  $^{12}\text{C}(n,n)$  between 2 and 6 MeV

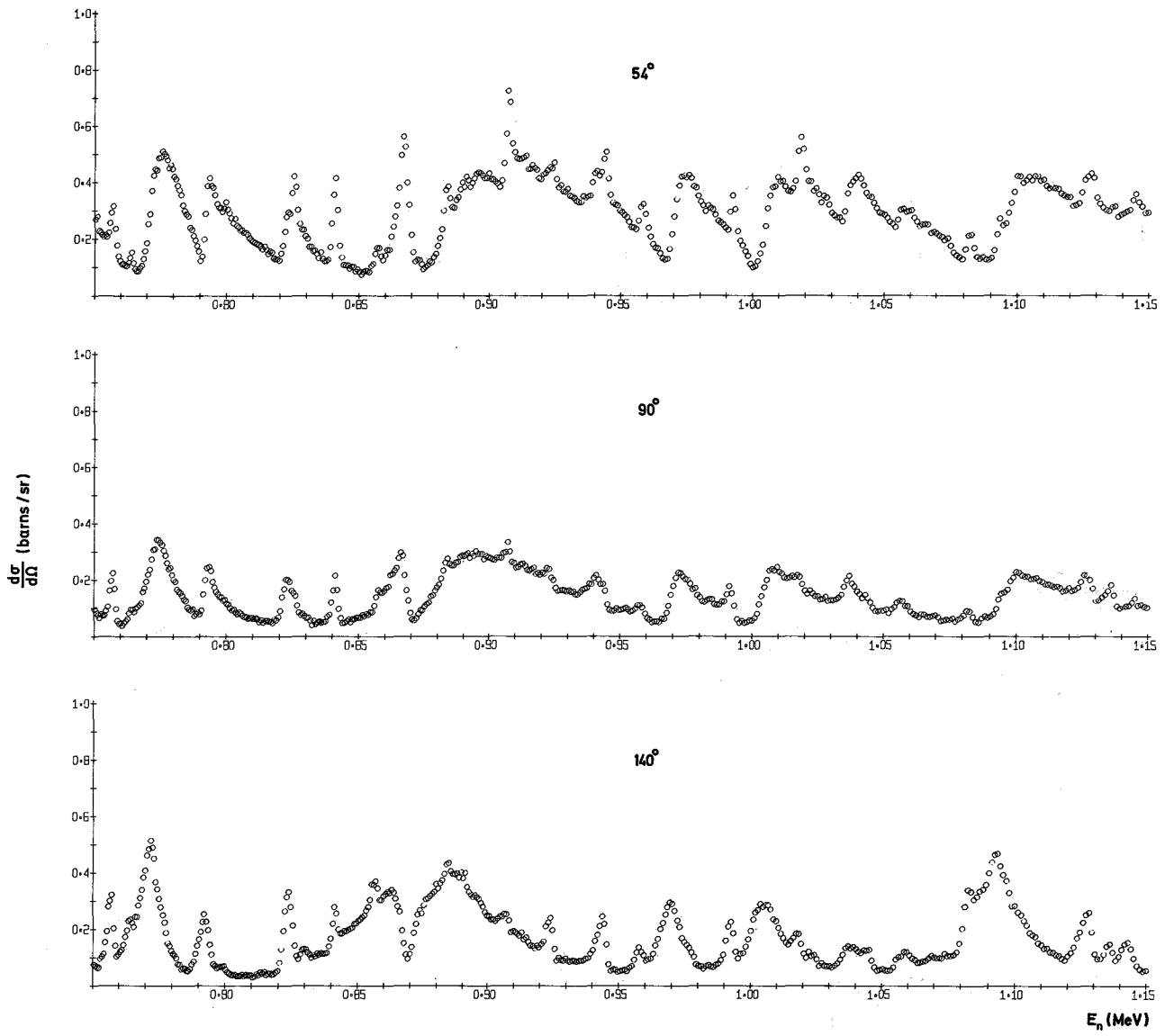


Fig.5 Differential Neutron Scattering Cross Section for  $^{40}\text{Ca}$  between 750 keV and 1.15 MeV

